


ENVIRONMENTAL RESEARCH
LETTERS

LETTER

Divergent trajectories of ocean warming and acidification

Eric Mortenson^{1,*} , Andrew Lenton^{1,2,3}, Elizabeth H Shadwick^{1,2,3}, Thomas W Trull¹,
Matthew A Chamberlain¹ and Xuebin Zhang^{1,3}¹ CSIRO Oceans & Atmosphere, Hobart, Australia² Australian Antarctic Program Partnership (AAPP), University of Tasmania, Hobart, Australia³ Centre for Southern Hemisphere Oceans Research (CSHOR), Hobart, Australia

* Author to whom any correspondence should be addressed.

E-mail: ericthemort@gmail.com**Keywords:** climate change, ocean biogeochemical model, ocean warming and acidificationSupplementary material for this article is available [online](#)

OPEN ACCESS

RECEIVED
6 July 2021REVISED
11 November 2021ACCEPTED FOR PUBLICATION
25 November 2021PUBLISHED
14 December 2021Original content from
this work may be used
under the terms of the
[Creative Commons
Attribution 4.0 licence](#).Any further distribution
of this work must
maintain attribution to
the author(s) and the title
of the work, journal
citation and DOI.

Abstract

The ocean provides a major sink for anthropogenic heat and carbon. This sink results in ocean changes through the dual stressors of warming and acidification which can negatively impact the health of the marine ecosystem. Projecting the ocean's future uptake is essential to understand and adapt to further climate change and its impact on the ocean. Historical ocean uptake of heat and CO₂ are tightly correlated, but here we show the trajectories diverge over the 21st century. This divergence occurs regionally, increasing over time, resulting from the unique combination of physical and chemical drivers. We explored this relationship using a high-resolution ocean model and a 'business as usual' CO₂ emission pathway, and demonstrate that the regional variability in the carbon-to-heat uptake ratios is more pronounced than for the subsequent carbon-to-heat storage (change in inventory) ratios, with a range of a factor of 30 (6) in heat-to-carbon uptake (storage) ratios among the defined regions. The regional differences in heat and carbon trajectories result in coherent regional patterns for sea surface warming and acidification by the end of this century. Relative to the mean global change (MGC) at the sea surface of 2.55 °C warming and a decrease of 0.32 in pH, the North Pacific will exceed the MGC for both warming and acidification, the Southern Ocean for acidification only, and the tropics and midlatitude northern hemisphere will exceed MGC only for warming. Regionally, mapping the ocean warming and acidification informs where the marine environment will experience larger changes in one or both. Globally, the projected ocean uptake of anthropogenic heat and carbon informs the degree to which the ocean can continue to serve as a sink for both into the future.

1. Introduction

The global oceans have taken up about 30% of the total anthropogenic carbon emissions [1, 2] and more than 90% of anthropogenic heat since preindustrial times [3, 4]. Projecting the efficacy of oceanic uptake into the future, for both heat and carbon, is central to predicting and understanding the future climate, and for developing policy to limit or adapt to climate change. While oceanic uptake provides a buffer for climate change through heat and carbon uptake, the resulting oceanic storage (i.e. change in content) of both anthropogenic heat and carbon is associated with negative consequences to the

marine environment through the dual stressors of heating and acidification [5, 6]. These impacts will vary regionally, affecting marine ecosystems with differing degrees of severity [7].

Although the air-sea exchange of heat and carbon both similarly depend on windspeed and air-sea gradients, there are several other mechanisms that can lead to differences in uptake and storage within the ocean. These include:

- (a) Ocean buffering capacity: The chemical buffering capacity of seawater for CO₂ partial pressure (pCO₂) is a nonlinear function of the concentration of total inorganic carbon, with a decrease, or

- slowed, carbon uptake capacity of the global oceans under increasing carbon emissions.
- (b) Vertical gradients: Temperature in most of the global ocean generally decreases with depth, as opposed to the gradient for carbon which increases with depth. Thus, while vertical mixing almost always enhances heat uptake, deep mixing associated with the meridional overturning circulation, generally ventilates carbon-rich deep waters, reducing the air-sea gradient of CO₂.
 - (c) Mesoscale features: Ocean eddies and western boundary currents serve to transport chemical and physical properties (e.g. [8]), but the limited horizontal resolution in many models means that these are not explicitly or well resolved. western boundary currents in particular are a major driver of poleward transport in the upper ocean, with opposing effects on air-sea heat and carbon exchange [9]. As these currents travel poleward, warm water releases heat to the colder atmosphere, enhancing ocean carbon uptake through solubility.
 - (d) Biological carbon export: The biological carbon pump reduces the concentration of total carbon in the near-surface ocean through primary production and exports a portion of this carbon to depth in organic form (export production). This sinking and remineralization of organic material has a substantial effect on the global ocean distribution of carbon, e.g. [10, 11].

In particular important mesoscale features such as western boundary currents and eddies are resolution-dependent and have often been overlooked especially in models incorporating biogeochemistry.

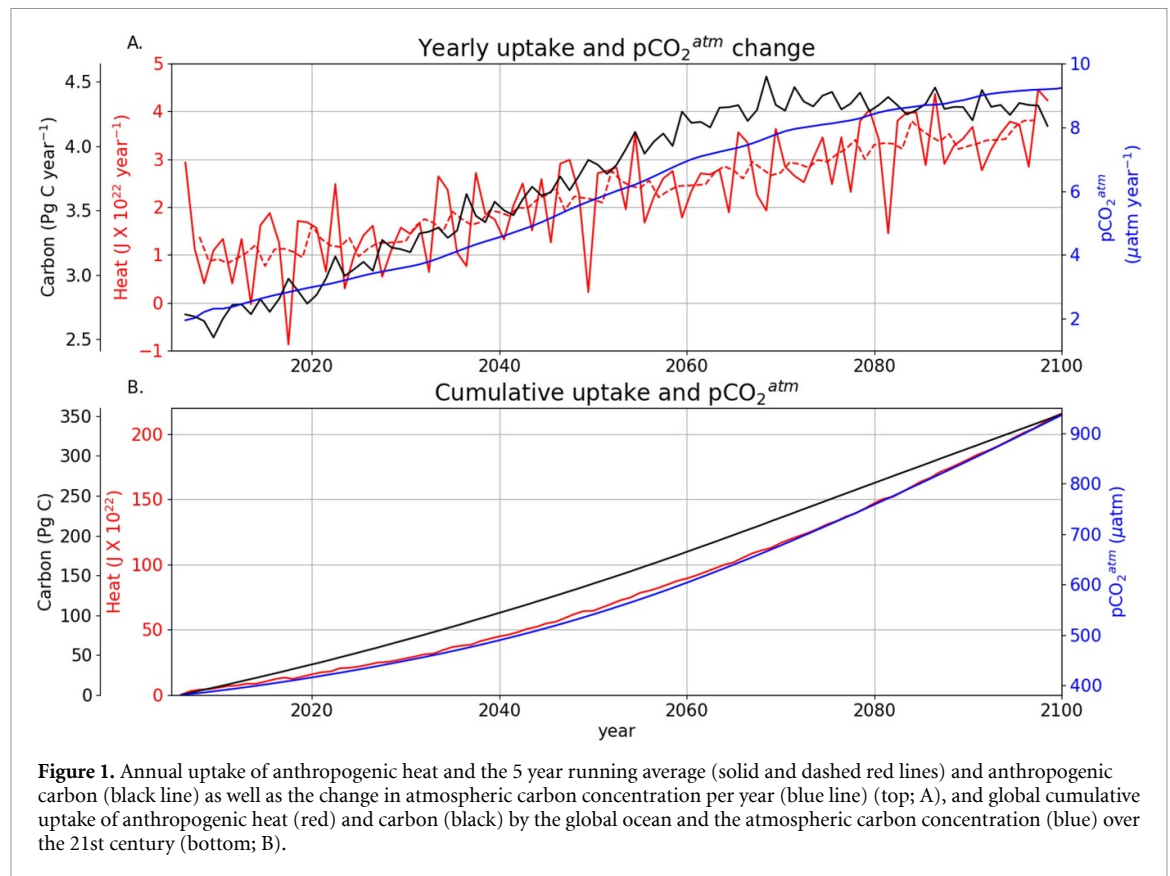
Although historically, the global ocean uptake of carbon and heat have been correlated, with the majority of anthropogenic heat and carbon over the Industrial Era ending up in the Southern Ocean [12], the mechanisms listed above (1–4) imply that this correlation is not causal. Other studies have shown that changes in circulation patterns affect the transport of carbon and heat differently, with redistribution of heat being more pronounced than carbon [13–15]. Furthermore, historical studies like [12], and many others looking at either historical or projected changes in ocean heat and/or carbon (e.g. [6, 13, 16–20]) typically have not resolved mesoscale circulation features. However, there are several studies that demonstrate the need for higher resolution in ocean simulations [21], found that representing anthropogenic carbon sequestration in the Southern Ocean requires a mesoscale-resolving simulation in order to capture the necessary transport processes involved. This is consistent with recent studies, notably [22–24], who highlighted the importance of resolving the mesoscale in simulating boundary currents and associated poleward and vertical tracer transports. In particular, studies that focus on the comparison of ocean pathways for heat and carbon

may underestimate their differences when mesoscale processes such as boundary currents are not resolved (e.g. [13]). In fact, mesoscale processes account for a substantial proportion of the kinetic energy of the surface ocean, comparable to and often more than that of the time-averaged ocean circulation [25]. These mesoscale processes have important contributions to the transport of heat [24] as well as biogeochemical tracers including carbon [26]. Despite the importance of resolving mesoscale features in the ocean, there are very few studies that utilize high-resolution models to study the effects on ocean uptake, transport, and/or storage of both heat and carbon, and those that do are generally regional studies rather than global (e.g. the Southern Ocean as in [15]).

The aim of this study is to utilize a high-resolution (0.1°) ocean-biogeochemical model [27] to determine the projected relationship between ocean heat and carbon uptake and storage. Recent work has highlighted the importance of simulating mesoscale processes in representing ocean variability and change [23, 24, 28]. Consequently, we have chosen to use a model that resolves the mesoscale in order to capture physical processes relevant to heat and carbon uptake and transport. The experiment and model setup are described in [27], with comparison to biogeochemical observations presented in [29]. The model has been evaluated in multiple regions with enhanced mesoscale energy, including boundary current systems around Australia [30], in the Indonesian Through Flow [31], the Southern Ocean [21], and along global Western boundary currents [22]. Specifically, we assess when, where, and by how much the oceanic uptake and storage of anthropogenic heat and carbon will distinctly evolve over the 21st century. We also use these projections to identify the oceanic distribution of stressors on marine ecosystems in terms of ocean heating, ocean acidification, or both.

2. Experimental setup

In this study, an ocean general circulation model, the Ocean Forecasting Australian Model, version 3 (OFAM3), is analyzed in an eddy-rich, 0.1° resolution over a near-global domain (75° N to 75° S). The ocean model OFAM3 is based on version 4.1 of the Modular Ocean Model [29, 32], and was designed to capture high-resolution upper ocean processes. The model has been calibrated to accurately represent air-sea heat exchange while minimizing drift in the ocean heat content [27]. The model does not explicitly treat sea ice, but is dependent on a prescribed Japanese 55 year Reanalysis product (JRA-55 [33]); sea ice coverage field, with the strength of atmospheric forcing dependent on the fraction of sea ice cover (see [27] for further detail).

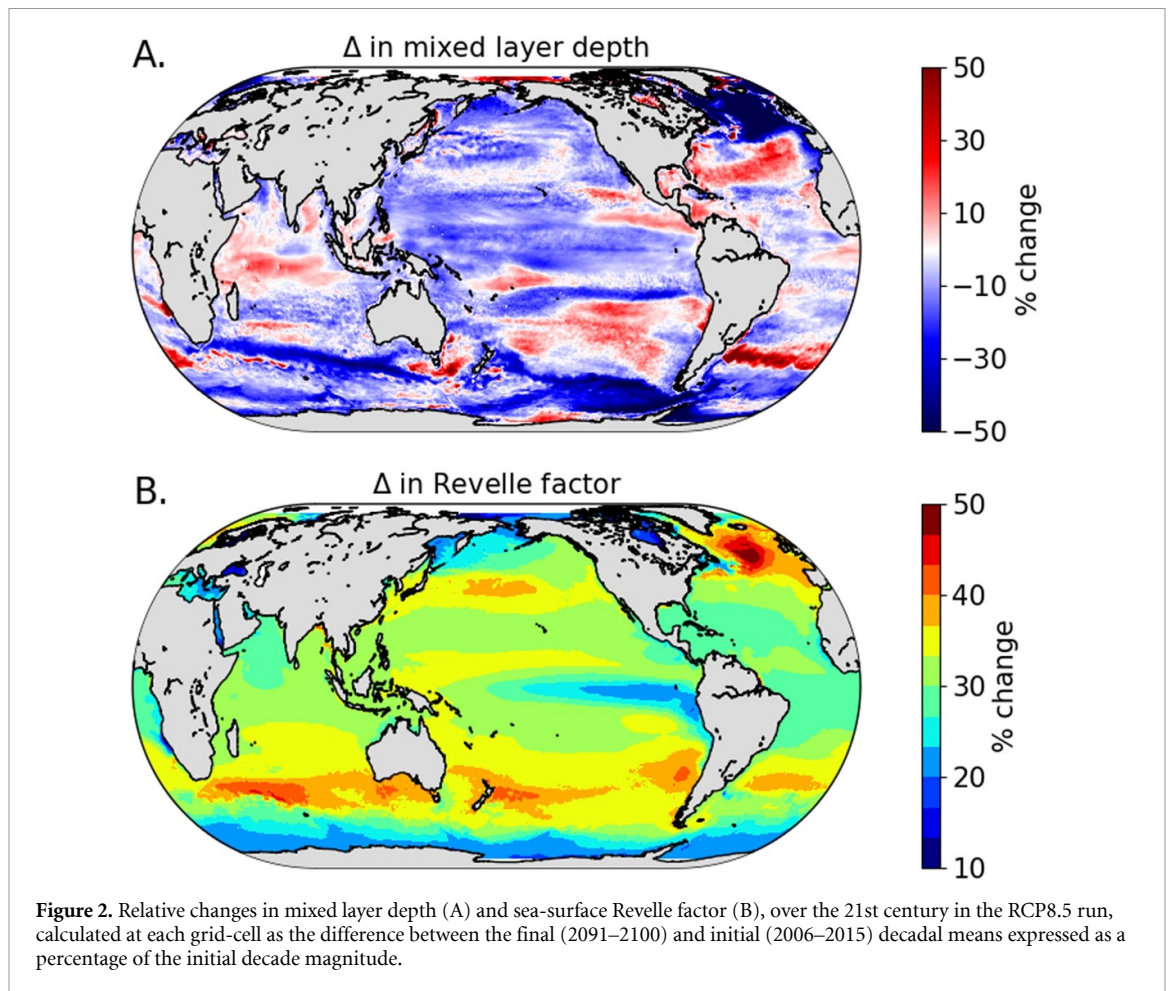


The model incorporates biogeochemistry through the Whole Ocean Model with Biogeochemistry and Trophic-dynamics, described in detail in [29]. It includes an ecosystem comprised of one phytoplankton group, dependent on light, phosphate, and iron, and one zooplankton group. The oceanic carbon system is dependent on biology and a wind-dependent air-sea exchange [34]. The initial conditions for dissolved inorganic carbon and total alkalinity based on the Global Ocean Data Analysis Project [35] and adjusted for the year 1997, as described in [29]. Phosphate and oxygen were initialized from the World Ocean Atlas [36, 37], phytoplankton is initialized with SeaWiFS climatology, zooplankton as a fraction (0.05) of phytoplankton, and iron from a 500 year coarse resolution biogeochemical model integration [29].

The design of the OFAM3 experiment includes a Control run, in which the atmospheric pCO₂ is kept at a constant preindustrial value of 280 ppm and the atmospheric forcing is a repeating 1979 annual cycle; and an RCP8.5 run, in which the atmospheric pCO₂ is prescribed to increase from 381 ppm in 2006 to 936 ppm by 2100 and the atmospheric forcing is based on the JRA-55 combined with RCP8.5 climate anomalies in atmospheric forcing fields, calculated from an ensemble of 17 CMIP5 models (see [27, 38] for details).

3. Results and discussion

Globally, the ocean uptake of anthropogenic heat continues to accelerate throughout the 21st century from 1×10^{22} J per year over the first decade (2006–2015) to 3.5×10^{22} J per year by the final decade (2091–2100) (figure 1(A), red), consistent with a multi-model mean of CMIP5 projections under RCP8.5 described in [16]. In terms of anthropogenic carbon, the uptake rate initially accelerates from around 2.75 PgC per year, but then levels off to a relatively constant rate of 4.25 PgC per year over the last 30 years of the century (figure 1(A), black), despite a continuing increase in the air-sea gradient of CO₂ (figure 1(A), blue). This is consistent with Earth System Model projections under RCP8.5 (e.g. [39]). The first decade of the modelled ocean subjected to RCP8.5 forcing shows a sensitivity to that forcing in annual global carbon uptake at the upper end of, but consistent with, current CMIP5 and CMIP6 models [40]. Integrating the anthropogenic heat and carbon uptake over the 21st century leads to a cumulative uptake of more than 2×10^{24} J of anthropogenic heat, and 350 Pg anthropogenic carbon (figure 1(B)). The global projection in this study is slightly less than the increase in heat among a multimodel ensemble mean under RCP8.5 forcing of 2.2×10^{24} J, as described in [16] (attributable to the volcanic forcing embedded

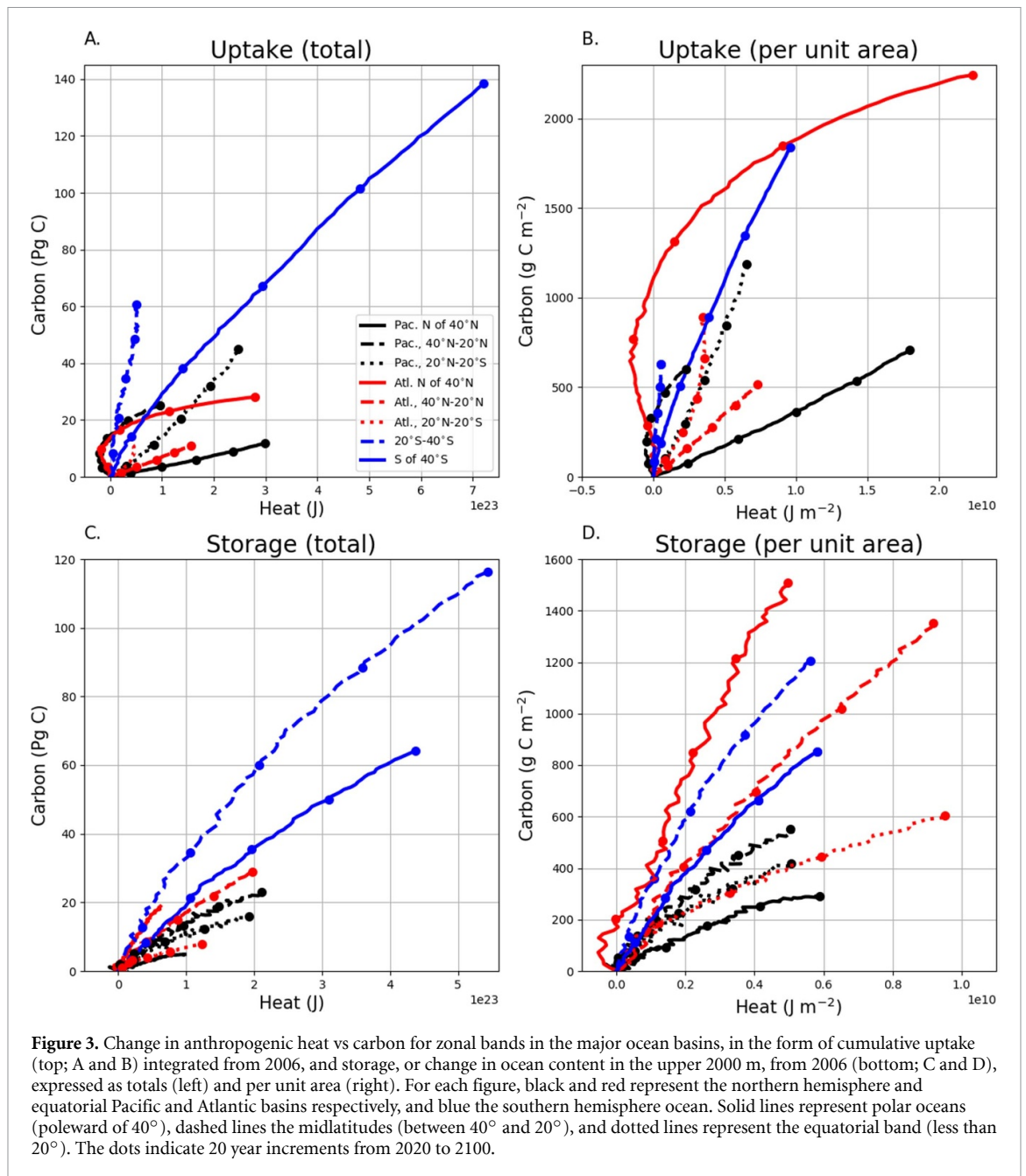


in the repeated interannual forcing in the present study, which is absent in the CMIP5 future simulations), and slightly below the CMIP5 multi-model mean ocean uptake of carbon with 400 PgC into the ocean over the period 2012–2100 (but with considerable uncertainty, with a range almost as large as the mean at 320–635 PgC, see table 6.12 and figure 6.24 of [41]). This projected ocean uptake equates to around a 10-fold increase in the anthropogenic heat and 4-fold increase in the anthropogenic carbon taken up by the oceans relative to the period 1870–1995 [12].

The global oceans exhibit substantial regional changes under RCP8.5 forcing that affect the uptake of heat and carbon. These include mixed layer depth (figure 2(A)), affecting the uptake of both heat and carbon, and the chemical property of carbon buffering capacity (figure 2(B)), represented by the Revelle factor [42], which is inversely proportional to the carbon buffering capacity. Here, we classify the anthropogenic change in the mixed layer depth and Revelle factor as the difference between the first and last decades in our RCP8.5 forcing scenario. The differing trajectories over time between the global ocean uptake of anthropogenic heat (consistently accelerating) and carbon (reaching a constant rate by the last third of the 21st century) reflect the reduction

in carbon uptake capacity of the global oceans under a high-emission scenario. The North Atlantic Ocean and the Southern Ocean exhibit enhanced shoaling of the mixed layer depth over the 21st century, and also an increase in Revelle factor, both of which would serve to weaken the carbon uptake capacity of the regions.

The oceanic response to anthropogenic emissions (figures 3(A) and (B)) can be divided into zonal bands representing high latitudes (poleward of 40°), intermediate latitudes (between 10° and 40°), and low/equatorial latitudes (less than 10°), and major basins within these. Consistent with current analyses, the southern hemisphere continues to dominate uptake of anthropogenic heat [43] and carbon [44]. The Southern Ocean south of 40°S takes up more than 7×10^{23} J of anthropogenic heat and nearly 140 PgC of anthropogenic carbon over the century (approximately one third of the global ocean uptake for heat and 40% for carbon; figure 3(A)). The ratio of regional anthropogenic carbon vs heat uptake is represented by the slopes (defined as the straight-line slope between the beginning and end of the respective trajectories), and there is a 30-fold range in slopes in uptake, with the highest carbon-to-heat uptake in the midlatitude Southern Ocean and the lowest in the North Pacific. The highest



uptake per unit area for both anthropogenic heat and carbon is in the Atlantic Ocean north of 40°N (figure 3(B)). This increase occurs despite an initial negative trajectory for anthropogenic heat uptake due to a projected slowdown of the Gulf Stream, which is compensated for by the strengthening ocean heat uptake later in the century. The associated Atlantic Meridional Overturning Circulation decreases almost linearly from 2020 to the end of the century in the RCP8.5 experiment, but the effect on the anthropogenic heat uptake (weakening) is apparently not as strong as the effect of the increasing regional air-sea temperature gradient (strengthening ocean heat uptake). The Southern Ocean south of 40°S has the second highest uptake of anthropogenic carbon per unit area while the Pacific Ocean north of

40°N has the second highest uptake of anthropogenic heat.

Both anthropogenic carbon and heat taken up at the surface are subject to transport processes once they have entered the ocean. We define the subsequent change in water column inventory over the 21st century as storage, shown in figures 3(C) and (D). The storage is calculated as the difference in the mean content between the first and last decades of the simulation (respectively, 2006–2015 and 2090–2099). Use of 30 year initial and final periods (not shown) shows similar results. The intermediate-latitude southern-hemisphere ocean (20° to 40°S) is projected to undergo the largest change in storage of any region (figure 3(C)), as the destination of the majority of anthropogenic heat and carbon taken

up at the sea surface further south, with more than 5.5×10^{23} J of anthropogenic heat and almost 120 Pg of anthropogenic carbon. The Southern Ocean south of 40°S has the second largest storage of both anthropogenic heat (4.5×10^{23} J) and carbon (65 PgC). The large storage of both anthropogenic heat and carbon in the southern hemisphere oceans is consistent with historical estimates ([43, 45] for heat [46, 47], for carbon, and [12] for both). Each of the remaining ocean regions are projected to contain less than half of the total storage, for either heat or carbon, than the Southern Ocean south of 40°S .

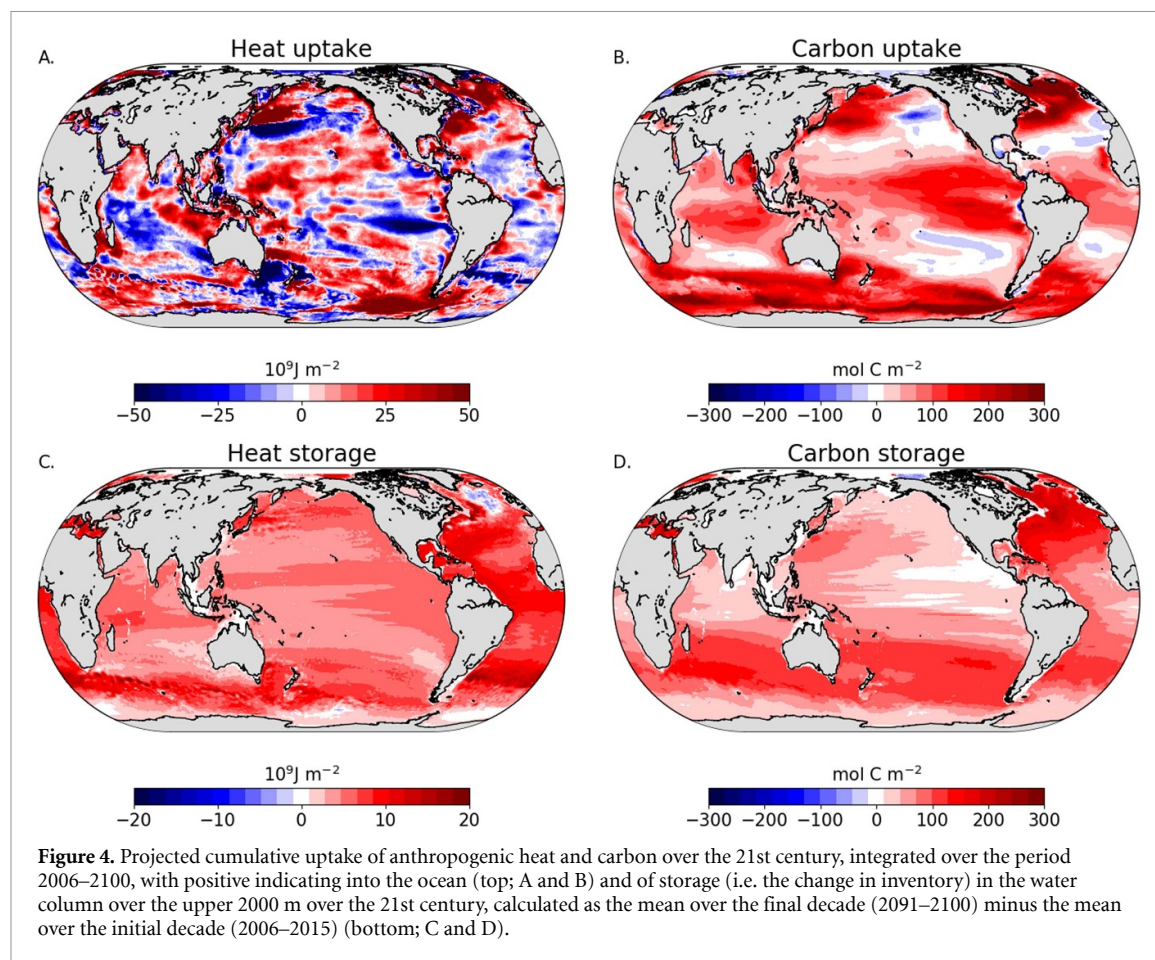
The relative trajectories of heat versus carbon storage per unit area (figure 3(D)) show that for all defined regions, the relationship is generally linear (indicating a constant carbon-to-heat storage ratio), but with varying slopes. This is true even for the North Atlantic, despite the non-linear trajectory of the cumulative surface uptake of anthropogenic heat and carbon (figures 3(A) and (B)). These slopes indicate a region-specific relationship between heat and carbon storage, as opposed to [13], who prescribe a single global-ocean ratio, or slope, for heat-to-carbon storage. These regional-specific linear heat-to-carbon storage slopes also suggest observations of both heat and carbon in the water column may be used to reinforce one another, as measurements from one can inform changes in the other. The variation in the magnitude of the slopes in the present study is due to a combination of regionally-distinct surface properties and horizontal transport processes as described in regional cases below.

The two extrema in slopes for anthropogenic carbon vs heat storage per unit area occur in the North Pacific and North Atlantic, with the North Atlantic anthropogenic carbon-to-heat storage ratio six times higher than that in the North Pacific. The smallest slope occurs in the North Pacific due to a combination of chemical (low alkalinity, or weaker buffer capacity) and physical (shallow mixed layer, or small reservoir) characteristics [48]. The chemical characteristics of the North Pacific are themselves a product of both physics and biology, namely the long residence time of waters before surfacing in the region (a feature of the global overturning circulation) and the biogenic export of carbon to those deep waters over time. In contrast, regions such as the midlatitude and Southern Oceans, despite also having a relatively weak chemical buffering capacity, still exhibit high carbon-to-heat storage slopes. These regions are able to absorb more anthropogenic carbon because they have deeper mixed layers [47]. The large slope in the North Atlantic is due to the loss of heat relative to carbon across the northern boundary [27] and consistent with present-day watermass exchange between the Arctic and North Atlantic (e.g. [49]). The differences described above (North Pacific, midlatitude and polar southern hemisphere, and North Atlantic oceans) highlight the complex interplay between the chemical

and physical features controlling the regional trajectories of anthropogenic heat and carbon uptake and storage.

Variations in cumulative centennial uptake of anthropogenic heat and carbon are also heterogeneous at smaller scales (figures 4(A) and (B)), especially for anthropogenic heat, which displays adjacent regions of release and uptake along the Kuroshio, the East Australia Current, and the equatorial Pacific Ocean. In contrast, there is consistent uptake of anthropogenic carbon at the termini of all three major western boundary currents (the Kuroshio, the Gulf Stream and the East Australia Current) as well as in the eastern equatorial Pacific Ocean and throughout the Southern Ocean (figure 4(B)). It is worth noting that the enhanced carbon uptake in the Southern Ocean is coincident with increasing biological export over the 21st century (figure S1(A) (available online at stacks.iop.org/ERL/16/124063/mmedia)), implying a link between biology and the ocean uptake of anthropogenic carbon. Although the increase in biological export in the Southern Ocean is consistent with a multimodel study [50], the same study found wide disagreement among models throughout the rest of the global ocean. Outside of the Southern Ocean, the scale of the biological contribution, and the negligible correlation throughout the rest of the global ocean between the change in biological export and the change in surface uptake over the century in the RCP8.5 run (figure S1(B)) indicate that the changes in carbon uptake are dominated by physical and/or chemical processes rather than biological processes. As anticipated under the RCP8.5 scenario, the trend in anthropogenic heat and carbon storage (figures 4(C) and (D)) are positive throughout most of the ocean with the exception of the Atlantic Ocean. Here, the differences in the patterns of storage stand out, with the majority of anthropogenic carbon stored in the north, but anthropogenic heat storage distributed throughout most of the basin, except in regions of the northern margin. The patterns of storage in the North Atlantic Ocean are linked to the loss of heat to the Arctic, as described above, as well as enhanced uptake of carbon, and despite the enhanced uptake of heat, at the Gulf Stream extension, in line with [51] (for heat) and with [2] (for carbon). Disparities between storage and uptake are due to horizontal transport of the given tracer, i.e. a horizontally static ocean would have identical storage and uptake at any location.

These regionally distinct ratios for the pathways of heat and carbon stand in contrast to [13], which finds a strong spatial correlation between maps of projected storage of carbon and heat in the global oceans. Although we do not present submesoscale features explicitly, their effects are inherent in the resolution of the simulation, and the emergent basin-scale effects of submesoscale features (e.g. eddies and western boundary currents) contribute to regional

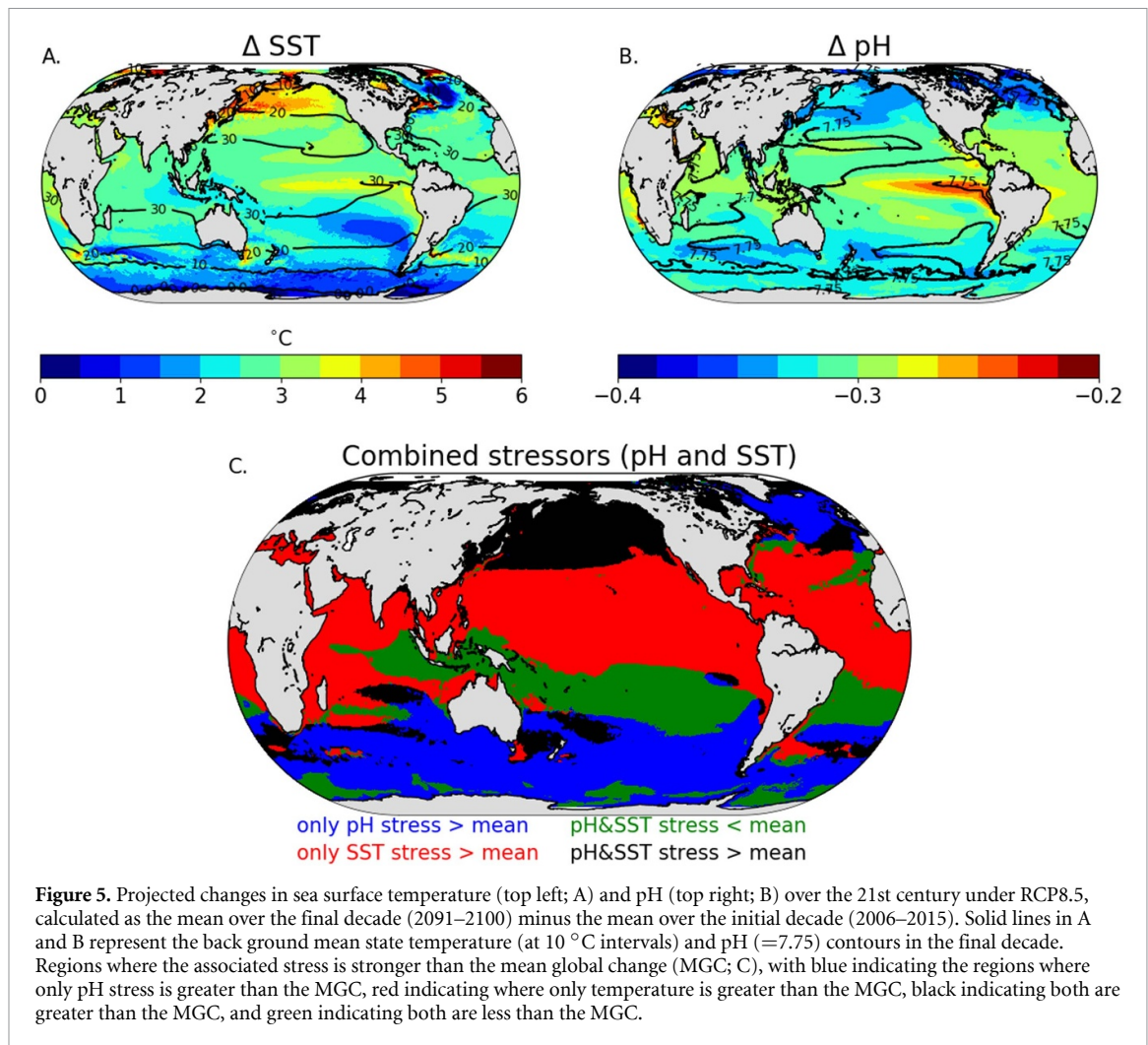


differences, not captured by the CMIP5 models analysed in [13]. These regional differences do not combine to produce a significantly different globally-integrated heat to carbon ocean storage ratio; the slightly higher ratio in our model ($6.9 \times 10^7 \text{ J mol}^{-1}$) in comparison to [13], is primarily attributable to our projection running further into the future.

The effects of heat and carbon uptake and storage over the 21st century are presented in terms of the changes to sea surface temperature (ΔSST) and pH (ΔpH) in order to illustrate regions of accelerated change in the upper ocean, similar to analysis in [20], along with a regional breakdown of where the change is dominated by heating and/or acidification described below. These surface changes differ somewhat from the distributions of uptake and storage, due to variations in subsurface transport, especially as it affects the vertical distributions of the added heat and carbon (shown through zonal mean vertical structure in figure S2). The intensity of surface warming over the 21st century in the RCP8.5 scenario is highest in northern and midlatitude oceans with little change in the Southern Ocean (figure 5(A)). In contrast, ΔpH is more intense at high latitudes in both hemispheres (figure 5(B)), consistent with ocean chemistry (e.g. [52]). The solid lines in figures 5(A) and (B) represent contours of the decadal means of SST and pH at the end of the 21st century under

RCP8.5 forcing, with the $\text{pH} = 7.75$ contour at the halfway point between the moderate ($\text{pH} 7.8\text{--}8$) and most intense ($\text{pH} < 7.7$) regimes of stress on corals as described in [53].

To explore how the divergent pathways of anthropogenically-derived heat and carbon impact the environment, the ΔSST and ΔpH were mapped relative to the mean global change (MGC) for each, i.e. an increase of 2.55°C in ocean temperature and a decrease of 0.32 in pH over the 21st century in the RCP8.5 run (figure 5(C)). It should be noted that these changes relative to the MGC show where the sea surface is heating and acidifying more or less, but this does not always equate to stress on organisms, which can depend on the mean state and seasonal variance as well as the type of species (e.g. [54]), which is beyond the scope of this study. It is also important to note that, although changes in pH are commonly used to quantify ocean acidification, the logarithmic nature of pH (relative to the hydrogen ion concentration, i.e. $\text{pH} = -\log_{10}[\text{H}^+]$) means that changes in pH should include information about the mean state (e.g. [55]). The decadal-averaged mean state at the beginning and end of the century are presented in figure S4. The patterns of heating and acidification demonstrate substantial regional variability in their relative impacts, with large coherent areas of the ocean surface exhibiting stresses that are greater than the MGC



over the century for either heating, acidification, or both. The Southern Ocean undergoes relatively large decreases in pH, consistent with [52, 56–58], but smaller changes in temperature (less than 2 °C) due to the region's link to the deep ocean through the meridional overturning circulation (see e.g. [59].), where the total carbon is relatively high and ocean temperature is low. The North Atlantic, at the terminus of the Gulf Stream, also undergoes a rate of acidification faster than the MGC. The North Pacific undergoes a combination of enhanced Δ SST and Δ pH, both greater than the MGC, due to weak vertical mixing (see, for example, supplementary figure 5(A) of [31], showing an increase in stratification in the North Pacific by the end of the 21st century). The equatorial and northern subtropical zones also exhibit weak mixing but with a higher buffering capacity, leading to Δ SST larger than the MGC, but not for Δ pH, in most of these regions. Tropical zones south of the equator in the Pacific and Atlantic, and in the vicinity of the Indonesian throughflow will encounter more stable conditions, with both heating and acidification weaker relative to their respective MGC.

4. Conclusion

Projections of the air-sea uptake and redistribution of anthropogenic heat and carbon within the global ocean are central to understanding the evolution of the climate system, and how this may impact the marine environment and the ecosystem services that it provides. This is the first study analyzing future global projections over the 21st century for both ocean heat and carbon pathways in a high-resolution simulation, providing a reference to compare with simulations that do not resolve mesoscale features. We find global ocean heat uptake continues to accelerate but ocean uptake of carbon approaches a constant annual rate by the last third of the century, despite the continued increase in atmospheric CO₂. At the basin scale, the generally linear nature of the heat vs carbon storage trajectories implies that the ratio is constant for each of the defined regions, but the ratios vary between them. The constant, but regionally distinct, ocean storage ratios between anthropogenic heat and carbon have profound implications for observing system design, suggesting that characterizing and understanding the slope of this

relationship could allow observations of carbon or heat storage to substantiate one another. As a single realization, this study is necessarily limited in a way that non-mesoscale resolving model-ensemble studies are not, but we anticipate further studies utilizing high-resolution models that represent mesoscale processes that may support or refute these findings.

Regional differences in the warming and ocean acidification of surface waters are pronounced, revealing large coherent areas where either ΔSST or ΔpH is larger than the MGC over the 21st century, but not both. Specifically, the Southern Ocean will undergo stronger acidification, and the equatorial and northern subtropical oceans will encounter stronger warming. The stress from ocean heating and acidification on organisms will influence marine ecosystems [6] and therefore are important considerations for food security and the ecosystem services they provide. In particular, regions with relatively small changes to temperature and pH identified in this study have the potential to serve as refugia [60] from the large-scale anthropogenic changes occurring in the global ocean.

Data availability statement

The data that support the findings of this study are available upon reasonable request from the authors.

Acknowledgments

We would like to acknowledge the assistance of Richard Matear, Philip Boyd, and Tyler Rohr in the development of this manuscript. We would also like to express thanks to the anonymous reviewers for their comments and advice.

This research was supported by the Centre for Southern Hemisphere Oceans Research (CSHOR), a partnership between the Commonwealth Scientific and Industrial Research Organisation (CSIRO) and the Qingdao National Laboratory for Marine Science; and the Australian Antarctic Program Partnership through the Australian Government's Antarctic Science Collaboration Initiative.

ORCID iD

Eric Mortenson  <https://orcid.org/0000-0002-3282-4974>

References

- [1] Friedlingstein P et al 2020 Global Carbon Budget 2020 *Earth Syst. Sci. Data* **12** 72
- [2] Khatiwala S et al 2013 Global ocean storage of anthropogenic carbon *Biogeosciences* **10** 2169–91
- [3] Meyssignac B et al 2019 Measuring global ocean heat content to estimate the earth energy imbalance *Front. Mar. Sci.* **6** 432
- [4] Rhein M et al 2013 Observations: Ocean *International Panel on Climate Change Climate Change, 2013: The Physical Science Basis Contribution of Working Group I to the Fifth Assessment Report of the Intergovernmental Panel on Climate Change* Ch 3, ed T F Stocker et al (Cambridge: Cambridge University)
- [5] Orr J A et al 2020 Towards a unified study of multiple stressors: divisions and common goals across research disciplines *Proc. R. Soc. B* **287** 20200421
- [6] Kwiatkowski L et al 2020 Twenty-first century ocean warming, acidification, deoxygenation, and upper-ocean nutrient and primary production decline from CMIP6 model projections *Biogeosciences* **17** 3439–70
- [7] Hurd C L, Lenton A, Tilbrook B and Boyd P W 2018 Current understanding and challenges for oceans in a higher- CO_2 world *Nat. Clim. Change* **8** 686–94
- [8] Sun B 2019 Global meridional eddy heat transport inferred from Argo and altimetry observations *Nat. Sci. Rep.* **9** 10
- [9] Imawaki S, Bower A S, Beal L and Qiu B 2013 Western Boundary Currents *Ocean Circulation and Climate* (Elsevier) **103** 305–38
- [10] Basu S and Mackey K 2018 Phytoplankton as key mediators of the biological carbon pump: their responses to a changing climate *Sustainability* **10** 869
- [11] Khatiwala S, Schmittner A and Muglia J 2019 Air-sea disequilibrium enhances ocean carbon storage during glacial periods *Sci. Adv.* **5** 10
- [12] Frölicher T L, Sarmiento J L, Paynter D J, Dunne J P, Krasting J P and Winton M 2015 Dominance of the Southern Ocean in anthropogenic carbon and heat uptake in CMIP5 models *J. Clim.* **28** 862–86
- [13] Bronselaer B and Zanna L 2020 Heat and carbon coupling reveals ocean warming due to circulation changes *Nature* **584** 227–33
- [14] Winton M, Griffies S M, Samuels B L, Sarmiento J L and Frölicher T L 2013 Connecting changing ocean circulation with changing climate *J. Clim.* **26** 2268–78
- [15] Chen H, Morrison A K, Dufour C O and Sarmiento J L 2019 Deciphering patterns and drivers of heat and carbon storage in the Southern Ocean *Geophys. Res. Lett.* **46** 3359–67
- [16] Cheng L, Abraham J, Hausfather Z and Trenberth K E 2019 How fast are the oceans warming? *Science* **363** 128–9
- [17] Lovenduski N S, McKinley G A, Fay A R, Lindsay K and Long M C 2016 Partitioning uncertainty in ocean carbon uptake projections: internal variability, emission scenario, and model structure *Glob. Biogeochem. Cycles* **30** 1276–87
- [18] Friedlingstein P et al 2014 Uncertainties in CMIP5 Climate Projections due to Carbon Cycle Feedbacks *J. Clim.* **27** 511–26
- [19] Gillett N P, Arora V K, Matthews D and Allen M R 2013 Constraining the ratio of global warming to cumulative CO_2 emissions using CMIP5 simulations *J. Clim.* **26** 6844–58
- [20] Bopp L et al 2013 Multiple stressors of ocean ecosystems in the 21st century: projections with CMIP5 models *Biogeosciences* **10** 6225–45
- [21] Langlais C E et al 2017 Stationary Rossby waves dominate subduction of anthropogenic carbon in the Southern Ocean *Sci. Rep.* **7** 17076
- [22] Hayashida H, Matear R J, Strutton P G and Zhang X 2020 Insights into projected changes in marine heatwaves from a high-resolution ocean circulation model *Nat. Commun.* **11** 4352
- [23] Kiss A E et al 2020 ACCESS-OM2 v1.0: a global ocean–sea ice model at three resolutions *Geosci. Model Dev.* **13** 401–42
- [24] Griffies S M et al 2015 Impacts on ocean heat from transient mesoscale eddies in a hierarchy of climate models *J. Clim.* **28** 952–77
- [25] Rhines P B and Eddies M 2019 *Encyclopedia of Ocean Sciences* (Amsterdam: Elsevier) pp 115–27 (available at: <https://linkinghub.elsevier.com/retrieve/pii/B9780124095489116422>)
- [26] McGillicuddy D J 2016 Mechanisms of physical-biological-biogeochemical interaction at the oceanic mesoscale *Annu. Rev. Mar. Sci.* **8** 125–59

- [27] Zhang X *et al* 2016 A near-global eddy-resolving OGCM for climate studies *Geosci. Model Dev. Discuss.* **52** (available at: <https://gmd.copernicus.org/preprints/gmd-2016-17/>)
- [28] Chassignet E P *et al* 2020 Impact of horizontal resolution on global ocean–sea ice model simulations based on the experimental protocols of the Ocean Model Intercomparison Project phase 2 (OMIP-2) *Geosci. Model Dev.* **13** 4595–637
- [29] Oke P R *et al* 2013 Evaluation of a near-global eddy-resolving ocean model *Geosci. Model Dev.* **6** 591–615
- [30] Feng M *et al* 2016 Invigorating ocean boundary current systems around Australia during 1979–2014: as simulated in a near-global eddy-resolving ocean model *J. Geophys. Res. Oceans* **121** 3395–408
- [31] Feng M, Zhang X, Sloyan B and Chamberlain M 2017 Contribution of the deep ocean to the centennial changes of the Indonesian Throughflow: centennial Changes of the ITF *Geophys. Res. Lett.* **44** 2859–67
- [32] Griffies S, Schmidt M and Herzfeld M 2009 Elements of MOM4p1 *GFDL Ocean Group Technical Report No. 6* p 444
- [33] Kobayashi S *et al* 2015 The JRA-55 reanalysis: general specifications and basic characteristics *J. Meteorolog. Soc. Japan II* **93** 5–48
- [34] Wanninkhof R 1992 Relationship between wind speed and gas exchange over the ocean *J. Geophys. Res.* **97** 7373
- [35] Key R M *et al* 2004 A global ocean carbon climatology: results from global data analysis project (GLODAP) *Glob. Biogeochem. Cycles* **18** 23
- [36] Garcia H E, Locarnini R A, Boyer T P and Antonov J L 2006 World ocean atlas 2005, volume 3: dissolved oxygen, apparent oxygen utilization, and oxygen saturation NOAA Atlas NESDIS 63 (Washington, DC: US Government Printing Office)
- [37] Garcia H E, Locarnini R A, Boyer T P and Antonov J L 2006 World ocean atlas 2005, volume 4: nutrients (phosphate, nitrate, silicate) NOAA Atlas NESDIS 64 (Washington, DC: US Government Printing Office)
- [38] Zhang X, Church J A, Monselesan D and McInnes K L 2017 Sea level projections for the Australian region in the 21st century: Sea level projections for Australia *Geophys. Res. Lett.* **44** 8481–91
- [39] Moore J K, Lindsay K, Doney S C, Long M C and Misumi K 2013 Marine ecosystem dynamics and biogeochemical cycling in the community earth system model [CESM1(BGC)]: comparison of the 1990s with the 2090s under the RCP4.5 and RCP8.5 Scenarios *J. Clim.* **26** 9291–312
- [40] Séférian R *et al* 2020 Tracking improvement in simulated marine biogeochemistry between CMIP5 and CMIP6 *Curr. Clim. Change Rep.* **6** 95–119
- [41] Ciais P *et al* 2013 Carbon and other biogeochemical cycles *Climate Change 2013: The Physical Science Basis Contribution of Working Group I to the Fifth Assessment Report of the Intergovernmental Panel on Climate Change* Ch 6, ed T F Stocker *et al* (Cambridge: Cambridge University) p 106
- [42] Revelle R and Suess H E 1957 Carbon dioxide exchange between atmosphere and Ocean and the question of an increase of atmospheric CO₂ during the past decades *Tellus* **9** 18–27
- [43] Rathore S, Bindoff N L, Phillips H E and Feng M 2020 Recent hemispheric asymmetry in global ocean warming induced by climate change and internal variability *Nat. Commun.* **11** 2008
- [44] Gruber N *et al* 2019 The oceanic sink for anthropogenic CO₂ from 1994 to 2007 *Science* **363** 1193–9
- [45] Sallée J-B 2018 Southern Ocean warming *Oceanography* **31** 52–62
- [46] Sabine C L 2004 The Oceanic sink for anthropogenic CO₂ *Science* **305** 367–71
- [47] Sallée J-B, Matear R J, Rintoul S R and Lenton A 2012 Localized subduction of anthropogenic carbon dioxide in the Southern Hemisphere oceans *Nat. Geosci.* **5** 579–84
- [48] Yasunaka S, Mitsudera H, Whitney F and Nakaoka S 2021 Nutrient and dissolved inorganic carbon variability in the North Pacific *J. Oceanogr.* **77** 3–16
- [49] Carmack E C *et al* 2016 Freshwater and its role in the Arctic Marine System: sources, disposition, storage, export, and physical and biogeochemical consequences in the Arctic and global oceans *J. Geophys. Res. Biogeosci.* **121** 675–717
- [50] Laufkötter C *et al* 2015 Drivers and uncertainties of future global marine primary production in marine ecosystem models *Biogeosciences* **12** 6955–84
- [51] He C, Liu Z and Hu A 2019 The transient response of atmospheric and oceanic heat transports to anthropogenic warming *Nat. Clim. Change* **9** 222–6
- [52] Orr J C *et al* 2005 Anthropogenic ocean acidification over the twenty-first century and its impact on calcifying organisms *Nature* **437** 681–6
- [53] Fabricius K E *et al* 2011 Losers and winners in coral reefs acclimatized to elevated carbon dioxide concentrations *Nat. Clim. Change* **1** 165–9
- [54] Vargas C A *et al* 2017 Species-specific responses to ocean acidification should account for local adaptation and adaptive plasticity *Nat. Ecol. Evol.* **1** 0084
- [55] Fassbender A J, Orr J C and Dickson A G 2021 Technical note: interpreting pH changes *Biogeosciences* **18** 1407–15
- [56] Doney S C *et al* 2009 Mechanisms governing interannual variability in upper-ocean inorganic carbon system and air–sea CO₂ fluxes: physical climate and atmospheric dust *Deep Sea Res. II* **56** 640–55
- [57] Fabry V, McClintock J, Mathis J and Grebmeier J 2009 Ocean acidification at high latitudes: the bellwether *Oceanography* **22** 160–71
- [58] Feely R, Doney S and Cooley S 2009 Ocean acidification: present conditions and future changes in a High-CO₂ world *Oceanography* **22** 36–47
- [59] Ferrari R, Nadeau L-P, Marshall D P, Allison L C and Johnson H L 2017 A model of the ocean overturning circulation with two closed basins and a reentrant channel *J. Phys. Oceanogr.* **47** 2887–906
- [60] Hampe A, Rodríguez-Sánchez F, Dobrowski S, Hu F S and Gavin D G 2013 Climate refugia: from the last glacial maximum to the twenty-first century *New Phytol.* **197** 16–18